

Size Dependence of the Photo- and Cathodo-luminescence of $Y_2O_3:S:Eu$ Phosphors

Hye-Jin Sung, Ki-Young Ko,[†] Hyun Soo Kim,[†] Seok-Soon Kweon, Jong-Yun Park,
Young Rag Do,[†] and Young-Duk Huh^{*}

Department of Chemistry, Institute of Nanosensor and Biotechnology, Dankook University, Seoul 140-714, Korea

^{*}E-mail: ydhuh@dankook.ac.kr

[†]Department of Chemistry, Kookmin University, Seoul 136-702, Korea

Received March 13, 2006

$Y_2O_3:S:Eu$ phosphors were synthesized via solid-state reactions. $Y_2O_3:S:Eu$ phosphor particles of various sizes were obtained by varying the firing temperature and firing time. The photoluminescence properties of these $Y_2O_3:S:Eu$ phosphors were examined. In addition, the cathodoluminescence properties of the $Y_2O_3:S:Eu$ phosphors were examined for applied voltages of 3–8 kV. The relationship between the luminescence intensity and particle size of the $Y_2O_3:S:Eu$ phosphors was investigated. The photoluminescence and cathodoluminescence of the $Y_2O_3:S:Eu$ phosphors are affected differently by variations in particle size.

Key Words : Photoluminescence, Cathodoluminescence, $Y_2O_3:S:Eu$, CNT-FED

Introduction

$Y_2O_3:S:Eu$ is one of the most important red-emitting phosphors. $Y_2O_3:S:Eu$ has a higher luminous efficiency and better color saturation than $Y_2O_3:Eu$. $Y_2O_3:S:Eu$ is extensively used in cathode-ray tubes (CRTs) and field emission displays (FEDs). FEDs are believed to have significant potential for realizing thin, flat-panel displays with high contrast, wide view angle, and low power consumption. The materials and technology utilized in FEDs and CRTs are similar. The basic structure of a FED consists of two separate plates, one with phosphors and one with field emitters. Emitted electrons are attracted from the emitter tips through an electric field onto the back plate. Many researchers have studied synthetic methods and the cathodoluminescence (CL) properties of $Y_2O_3:S:Eu$ phosphors for use in low voltage (< 2 kV) Spindt-type FEDs.^{1–4} Carbon nanotubes (CNTs) have properties that are favorable to their use as field emitters in FEDs, such as a high aspect ratio, sharp tips, high chemical stability, and high mechanical strength.^{5–7} The operational voltage requirements of FEDs have changed from low voltages (< 2 kV) to middle voltages (3–8 kV), because CNT-FEDs use higher voltage electron beams than Spindt-type FEDs in order to obtain greater brightness and longer lifetimes.

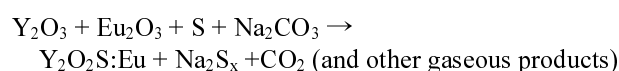
The advent of blue InGaN technology has made it possible to produce conventional white light emitting diodes (white LEDs), which produce white light from a yellow-emitting YAG:Ce phosphor coated onto a blue LED chip.^{8–11} White LEDs have a number of advantages over incandescent and halogen lamps, such as their power efficiency and long lifetime. However, the spectral composition of the light produced by conventional white LEDs differs from that of natural white light, particularly in the red region. Three-band white LEDs, in which blue-, green-, and red-emitting phosphors are coated onto near-UV LEDs or UV LEDs, offer better color properties.¹² $Y_2O_3:S:Eu$ has an absorption band up to 400 nm and so is considered to be a promising

candidate for use as a red-emitting phosphor excited by UV LEDs.¹³

However, there is limited information about the effects of the size of $Y_2O_3:S:Eu$ phosphors on their PL and CL properties. In this present study, $Y_2O_3:S:Eu$ phosphors of various sizes were synthesized via solid-state reactions. The variations of the PL and CL properties of the $Y_2O_3:S:Eu$ phosphors with particle size were investigated. We examined the CL properties of the $Y_2O_3:S:Eu$ phosphors at applied voltages of 3–8 kV to check their suitability for use as red-emitting phosphors in CNT-FEDs. The particle size dependence in CL brightness could be important information on phosphors morphology for CNT-FED device.

Experimental Section

Y_2O_3 (99.99%, Rhodia, 50 nm), Eu_2O_3 (99.99%, Aldrich), S (99.998%, Aldrich), Na_2CO_3 (Aldrich), and K_2HPO_4 (Aldrich) were used. The $Y_2O_3:S:Eu$ phosphors were prepared via solid-state reactions. The raw materials Y_2O_3 , Eu_2O_3 , and S were mixed with Na_2CO_3 and K_2HPO_4 as fluxes. The activator concentration was fixed at 6.0%. The weight ratio of $Y_2O_3/Eu_2O_3/S/Na_2CO_3/K_2HPO_4$ was 1.76 : 0.18 : 0.8 : 1.2 : 0.27. The mixed materials were fired at temperatures in the range 950–1250 °C for 4 h. The mixed materials were also fired at 1250 °C for various firing times in the range 1 min to 4 h. The phosphors were washed with water to remove the flux residue, then filtered and dried under vacuum at room temperature. The formation reaction of $Y_2O_3:S:Eu$ phosphors is as follows:



The structures of the $Y_2O_3:S:Eu$ phosphors were analyzed with powder X-ray diffraction (XRD, Phillips PW 1710) using $Cu K_{\alpha}$ radiation. The morphologies of the $Y_2O_3:S:Eu$ phosphors were characterized with scanning electron

microscopy (SEM, Phillips XL30 ESEM-FEG). The PL excitation and emission spectra were obtained by using a spectrum analyzer (DARSA II, PSI) with a 0.275 m monochromator, a photomultiplier tube, and a 500 W Xe lamp as the excitation source. The incident beam was perpendicular to the surface of the sample, and the observation angle was 45° relative to the excitation source. CL measurements were carried out in a high-vacuum (5×10^{-7} torr) chamber for various excitation energies. Patch-type samples were prepared on metal holders. The $Y_2O_2S:Eu$ phosphor patches were placed in a demountable cathode ray tube and excited with electron beams with various DC excitation energies. For the lifetime study, the CL intensities were measured as a function of time at 5 kV using DC and a peak current density of $3 \mu A/cm^2$.

Results and Discussion

Figure 1 shows the X-ray powder diffraction (XRD) patterns of $Y_2O_2S:Eu$ phosphors obtained by firing at temperatures between 950 and 1250 °C for 4 h. The XRD patterns match those in the JCPDS file for hexagonal Y_2O_2S (24-1424) with a unit cell characterized by $a = 3.81 \text{ \AA}$ and $c = 6.59 \text{ \AA}$. The europium ion is expected to occupy the yttrium site in $Y_2O_2S:Eu$, since the ionic radius of Eu^{3+} (0.95 Å) is slightly larger than that of Y^{3+} (0.89 Å).¹⁴ However, two minor peaks ($2\theta = 20.5^\circ$ and 29.1°) corresponding to the Y_2O_3 were observed in XRD pattern of $Y_2O_2S:Eu$ phosphor obtained by firing at 1250 °C. Figure 2 shows the SEM images of $Y_2O_2S:Eu$ obtained by firing at temperatures between 950 to 1250 °C for 4 h. The shapes of $Y_2O_2S:Eu$ particles depend on the kind of flux.¹⁵ Since Na_2CO_3 and K_2HPO_4 were used as fluxes in this study, nearly spherical particles were formed. The particle size increases with increases in the firing temperature. $Y_2O_2S:Eu$ particles fired at 950 °C have a size of about 500 nm, whereas $Y_2O_2S:Eu$ particles fired at 1250 °C have a size of 5 μm . $Y_2O_2S:Eu$ phosphors of various sizes were also synthesized by varying the firing

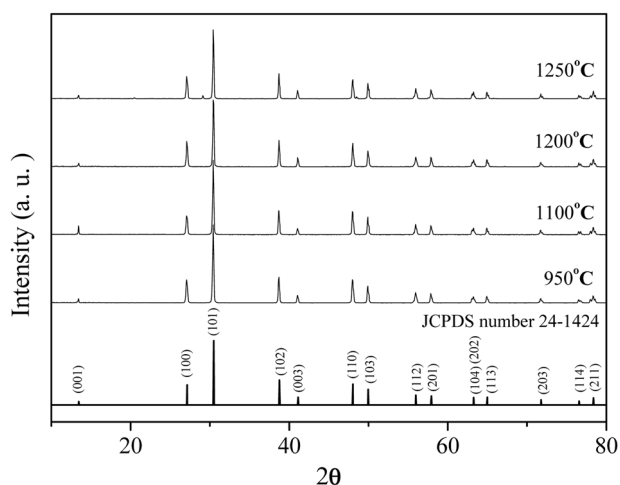


Figure 1. X-ray diffraction patterns of $Y_2O_2S:Eu$ phosphors obtained by firing at various temperatures for 4 h.

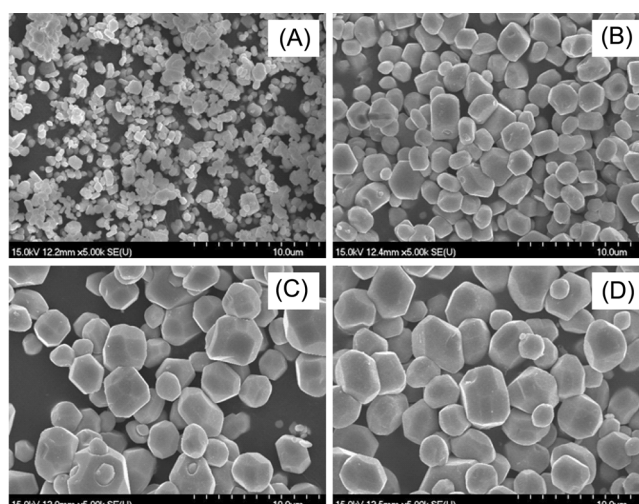


Figure 2. SEM images of $Y_2O_2S:Eu$ phosphors obtained by firing at various firing temperatures for 4 h: (A) 950 °C; (B) 1100 °C; (C) 1200 °C; (D) 1250 °C.

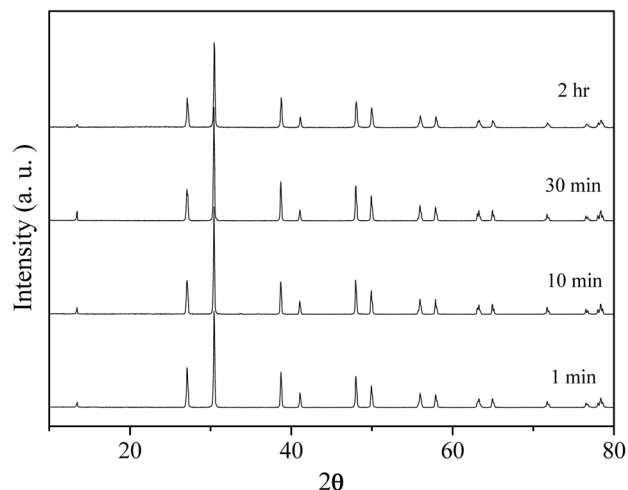


Figure 3. X-ray diffraction patterns of $Y_2O_2S:Eu$ phosphors obtained by various firing times at 1250 °C.

time at 1250 °C. The presence of single phase $Y_2O_2S:Eu$ was also confirmed from their XRD patterns. Figure 3 shows the XRD patterns of $Y_2O_2S:Eu$ phosphors obtained by various firing times at 1250 °C. The XRD patterns indicate that Y_2O_2S is formed even in short firing time. Figure 4 shows the SEM images of $Y_2O_2S:Eu$ obtained at 1250 °C for firing times from 1 min to 2 h. Larger particle sizes arise for longer firing times. Note that the $Y_2O_2S:Eu$ particles fired for 1 min and 2 h have an average size of about 1 μm and 3 μm respectively. Both the firing temperature and the firing time affect the growth of the $Y_2O_2S:Eu$ particles.

Figure 5 shows the PL spectra of $Y_2O_2S:Eu$ obtained by firing at temperatures ranging from 950 to 1250 °C for 4 h. The main emission peaks are due to the Eu^{3+} transition $^5D_J \rightarrow ^7F_J$. The stronger red emission lines at 626 and 617 nm are due to the transition $^5D_0 \rightarrow ^7F_2$. The deep red emission line at 706 nm is due to the transition $^5D_0 \rightarrow ^7F_4$. The shorter wavelength lines at 583, 587, and 595 nm correspond to the transitions

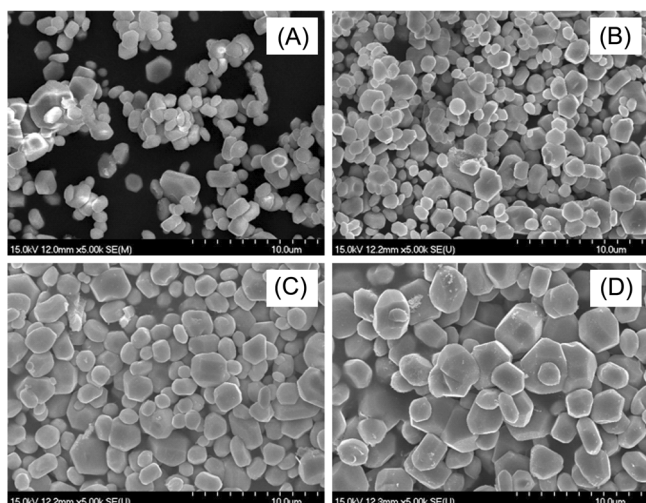


Figure 4. SEM images of $Y_2O_3:S:Eu$ phosphors obtained with various firing times at 1250 °C: (A) 1 min; (B) 10 min; (C) 30 min; (D) 2 h.

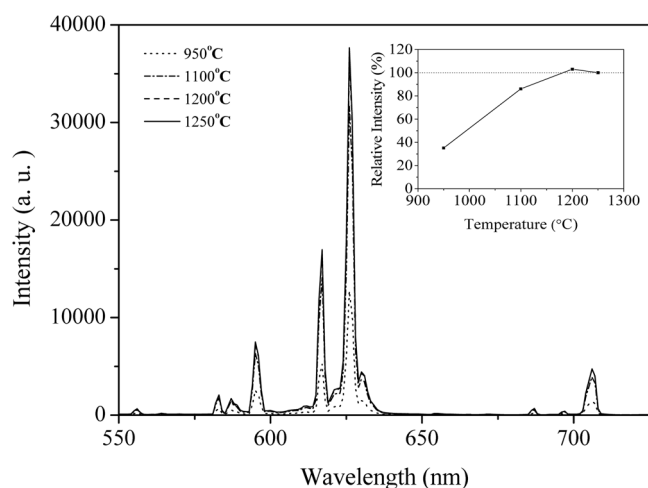


Figure 5. Emission spectra ($\lambda_{ex} = 365$ nm) of $Y_2O_3:S:Eu$ phosphors obtained by firing at various temperatures for 4 h. The inset shows the variation of the relative emission intensity with the firing temperature.

$^5D_0 \rightarrow ^7F_2$, $^5D_1 \rightarrow ^7F_1$, and $^5D_0 \rightarrow ^7F_1$, respectively.^{13,16} Note that as the firing temperature increases up to 1200 °C the strongest emission intensity at 626 nm also increases (see inset). However, the emission intensity at 626 nm of $Y_2O_3:S:Eu$ fired at 1250 °C is less than that of $Y_2O_3:S:Eu$ fired at 1200 °C, which can be explained by the minor formation of Y_2O_3 at 1250 °C. Figure 6 shows the photoluminescence excitation (PLE) spectra of $Y_2O_3:S:Eu$. The PLE spectra consist of extremely broad bands that extend well into the near-UV region. Therefore, $Y_2O_3:S:Eu$ can be used as a red-emitting phosphor in a three-band white LED excited by near-UV LEDs. The band below 300 nm is essentially due to the host lattice Y_2O_3 absorption. The broad band around 350 nm arises from the charge transfer transition between Eu^{3+} and anions (O^{2-} or S^{2-}). Figure 7 shows the PL spectra of $Y_2O_3:S:Eu$ obtained at 1250 °C with firing times of 1 min

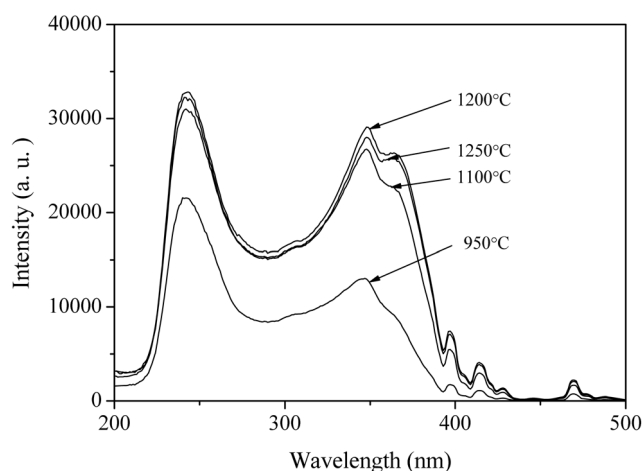


Figure 6. Excitation spectra ($\lambda_{em} = 626$ nm) of $Y_2O_3:S:Eu$ phosphors obtained by firing at various temperatures for 4 h.

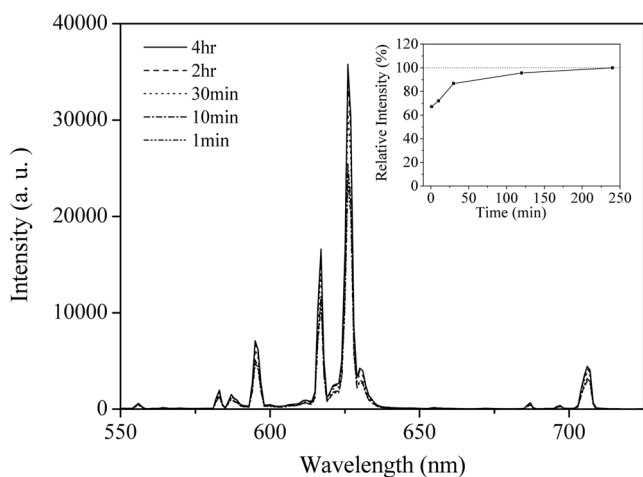


Figure 7. Emission spectra ($\lambda_{ex} = 365$ nm) of $Y_2O_3:S:Eu$ phosphors obtained with various firing times at 1250 °C. The inset shows the variation of the relative emission intensity with the firing time.

to 4 h. As shown in Figure 7, the emission intensity at 626 nm increases with increases in the firing time. The growth of $Y_2O_3:S:Eu$ particles depends on both firing temperature and firing time. The PL intensity also depends on the size of the phosphors. The $Y_2O_3:S:Eu$ particle sizes obtained by firing at 1250 °C for 30 min and at 1100 °C for 4 h are similar. The relative intensities of $Y_2O_3:S:Eu$ obtained by firing at 1250 °C for 30 min and at 1100 °C for 4 h are 86.8% and 86.1% respectively. This indicates that the PL intensity of a $Y_2O_3:S:Eu$ particle is roughly proportional to its size. Similar results are obtained by comparing the PL intensities of the $Y_2O_3:S:Eu$ particles obtained by firing at 1250 °C for 1 min and at 950 °C for 4 h. The particle size of $Y_2O_3:S:Eu$ obtained by firing at 1250 °C for 1 min is larger than that of $Y_2O_3:S:Eu$ obtained by firing at 950 °C for 4 h. $Y_2O_3:S:Eu$ obtained by firing at 1250 °C for 1 min has a brighter luminescence than $Y_2O_3:S:Eu$ obtained by firing at 950 °C for 4 h. This indicates that the PL intensity of a $Y_2O_3:S:Eu$ particle is roughly proportional to its size, but this does not apply to $Y_2O_3:S:Eu$ particle by firing at 1250 °C for 4 h. Most of phosphors show

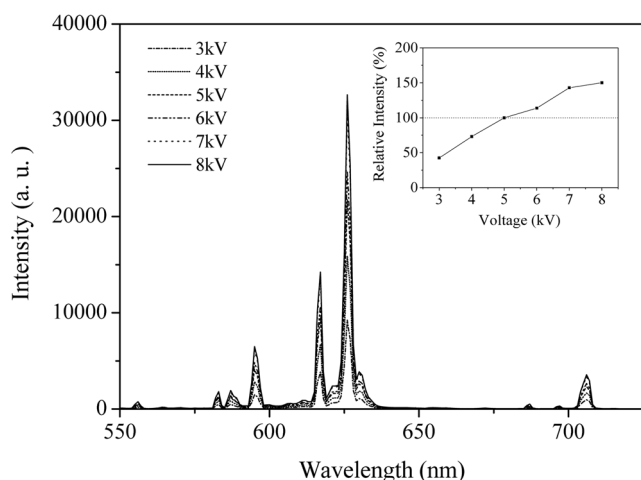


Figure 8. CL emission spectra of $\text{Y}_2\text{O}_2\text{S}:\text{Eu}$ phosphor fired at 1250 °C for 4 h for various applied voltages. The inset shows the variation of CL brightness with applied voltage.

their highest luminescence intensity for particle sizes of a few μm . The $\text{Y}_2\text{O}_2\text{S}:\text{Eu}$ particle obtained by firing at 1250 °C for 4 h has a size of 5 μm , which is the typical size of commercial phosphors.

The CL spectra of the $\text{Y}_2\text{O}_2\text{S}:\text{Eu}$ phosphor obtained by firing at 1250 °C for 4 h with applied voltages between 3 and 8 kV are in Figure 8, obtained under DC excitation with a current density of 3 $\mu\text{A}/\text{cm}^2$, and measured in reflection mode. The intensity of the strongest emission intensity, at 626 nm, increases with the excitation voltage. The inset shows the CL brightness-operating voltage curves, and the linear voltage dependence of the CL. The CL efficiency is roughly proportional to the applied voltage. The CL of $\text{Y}_2\text{O}_2\text{S}:\text{Eu}$ obtained by firing at 1250 °C for 4 h is 534.5 cd/m^2 at a voltage of 5 kV and a current density of 3 $\mu\text{A}/\text{cm}^2$. It has been estimated in previous publications that a red luminescence of 460 cd/m^2 is required in order to achieve the level of white required by a typical display, 200 cd/m^2 .¹⁷ The $\text{Y}_2\text{O}_2\text{S}:\text{Eu}$ phosphor at 5 kV voltage produces better CL efficiencies than those required for FEDs. Since CNT-FEDs are operated under more than 5 kV, $\text{Y}_2\text{O}_2\text{S}:\text{Eu}$ can be used as a red-emitting phosphor in CNT-FEDs.

The relative CL intensities of the $\text{Y}_2\text{O}_2\text{S}:\text{Eu}$ phosphors obtained under various firing conditions are shown as a function of applied voltage in Figure 9. The $\text{Y}_2\text{O}_2\text{S}:\text{Eu}$ phosphors obtained with three different firing conditions exhibit similar relative CL intensity dependences on the applied voltage. The firing conditions of the three $\text{Y}_2\text{O}_2\text{S}:\text{Eu}$ phosphors were 1250 °C for 4 h, 1250 °C for 1 min, and 950 °C for 4 h, with particle sizes of 5 μm , 1 μm , and 500 nm, respectively. These results indicate that the CL brightness is not affected by variation of the particle size of the $\text{Y}_2\text{O}_2\text{S}:\text{Eu}$ phosphors in the range 500 nm to 5 μm . Figure 10(A) shows the variation of the CL brightness of $\text{Y}_2\text{O}_2\text{S}:\text{Eu}$ with firing temperature at a voltage of 5 kV and a current density of 3 $\mu\text{A}/\text{cm}^2$. The firing temperature does not significantly affect the CL brightness. However, as the firing temperature

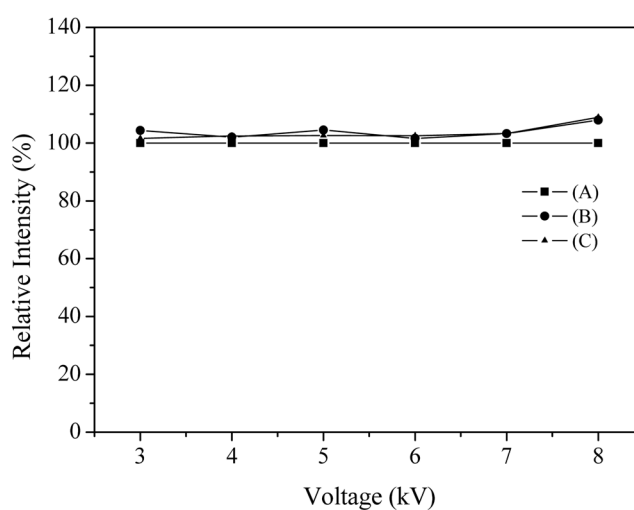


Figure 9. The relative CL intensities of $\text{Y}_2\text{O}_2\text{S}:\text{Eu}$ phosphors obtained with various firing conditions as a function of excitation voltage. (A) at 1250 °C for 4 h; (B) at 950 °C for 4 h; (C) at 1250 °C for 1 min.

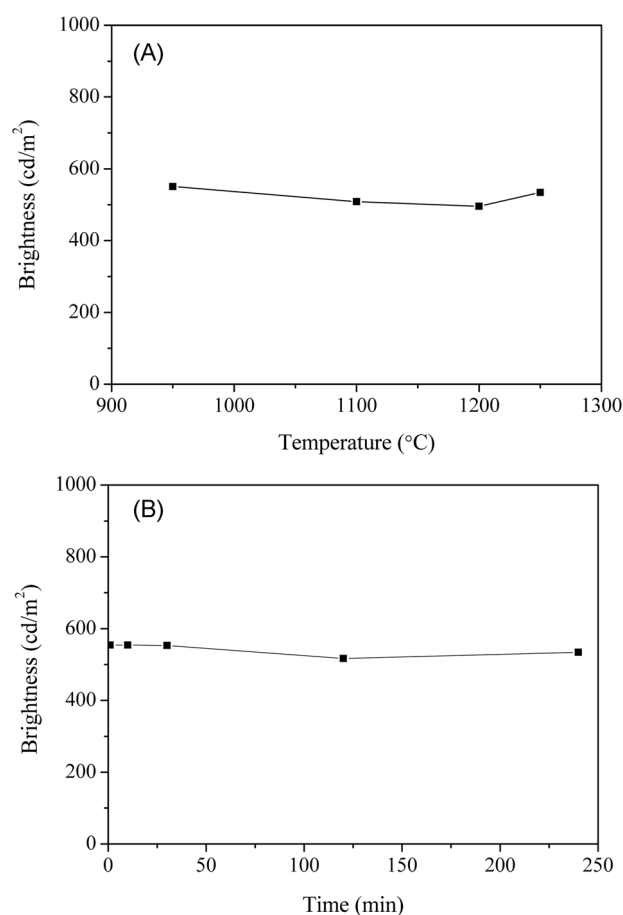


Figure 10. CL brightness of $\text{Y}_2\text{O}_2\text{S}:\text{Eu}$ phosphors as a function of (A) firing temperature and (B) firing time. The applied voltage and current are 5 kV and 3 $\mu\text{A}/\text{cm}^2$ respectively.

increases the PL intensity increases, as shown in the inset of Figure 5. Figure 10(B) shows the variation of the CL brightness of $\text{Y}_2\text{O}_2\text{S}:\text{Eu}$ with firing time. The firing time

does not significantly affect the CL brightness, whereas the PL intensity strongly depends on the firing time, as shown in Figure 7. The dependence of the PL and CL intensities on the size of the $Y_2O_3S:Eu$ particles are different because the mechanisms of PL and CL are different. An increasing in phosphor size coincides with a decrease in the ratio of surface area to phosphor volume. When the phosphors have perfect spherical shapes, the ratio of surface area to volume is simply proportional to the inverse of the radius of the phosphor. Surface defects produce nonradiative recombination processes of electrons and holes. The importance of surface defects depends on the ratio of surface area to phosphor volume. Therefore, the PL efficiency is expected to increase as the particle size increases.

The CL mechanism of $Y_2O_3S:Eu$ is known to be the recombination of electrons and holes at Eu^{3+} and Eu^{2+} . In the Y_2O_3S crystal, the Eu^{3+} ion traps an electron and is converted to Eu^{2+} , producing a negatively charged local field. A hole is attracted to this region and is captured, forming excited state Eu^{3+} . The excited Eu^{3+} emits a photon and returns to the ground state of Eu^{3+} .¹⁸ However, CL behavior in CRTs is slightly different to that in FEDs due to the penetration depth of the phosphor. The penetration depth in CNT-FEDs is much less than that in CRTs, since the applied voltage of 5 keV used in CNT-FED is smaller than that used in CRTs, 27 keV. The relationship between penetration depth and applied voltage in the range 1-10 keV can be expressed with the Feldman equation as follows:¹⁹

$$R(\text{\AA}) = 250 \left(\frac{A}{\rho} \right)^{\frac{n}{2}} Z^2 E^n, \quad n = 1.2 / (1 - 0.29 \log Z)$$

where R , A , ρ , Z , and E are the penetration depth, molecular mass, density, sum of atomic numbers in the molecule, and applied voltage in keV, respectively. The calculated penetration depths for the Y_2O_3S crystal at 3, 5, and 8 keV are 33, 147, and 450 nm, respectively. The firing conditions of the three $Y_2O_3S:Eu$ phosphors were 1250 °C for 4 h, 1250 °C for 1 min, and 950 °C for 4 h, which produced particle sizes of 5 μm , 1 μm , and 500 nm, respectively. Since the penetration depth is much less than the particle size (5 μm), most of the volume in the phosphor is not excited by electrons. In fact, only the volume in near the surface is excited by electrons. In this situation, small particles can be packed more densely than large particles. The increased proportion of the volume of small particles that is excited by electrons gives rise to an increase in the emission. However, the ratio of surface area to phosphor volume is higher for small particles, which decreases the emission. The positive and negative effects on CL behavior occur simultaneously as the particle size decreases. Therefore, the CL efficiency does not depend strongly on the particle size. However, if photons penetrate through the phosphor, negative effects on the PL efficiency can dominate with decreases in the particle size.

The lifetime decay behavior of the $Y_2O_3S:Eu$ phosphors was also measured under 5 kV electron excitation with an average current density of 3 $\mu\text{A}/\text{cm}^2$. Figure 11 shows the decay curves of the $Y_2O_3S:Eu$ phosphors obtained with three

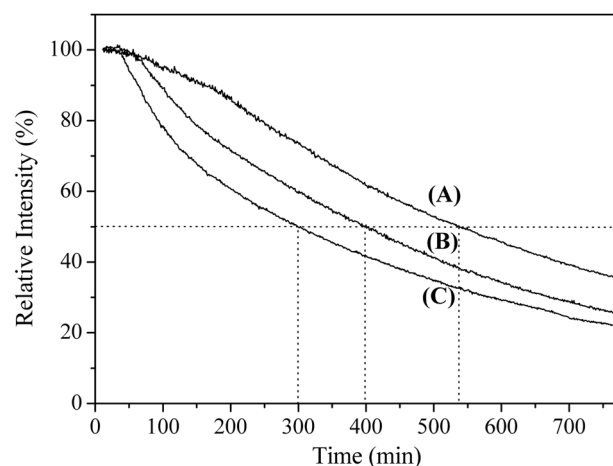


Figure 11. CL lifetime decay curves of $Y_2O_3S:Eu$ phosphors obtained for various firing conditions. (A) at 1250 °C for 4 h; (B) at 950 °C for 4 h; (C) at 1250 °C for 1 min.

different firing conditions. The three $Y_2O_3S:Eu$ phosphors have particle sizes of 5 μm , 1 μm , and 500 nm, and their lifetimes were found to be 536 min, 299 min, and 399 min, respectively. The lifetime of a phosphor is generally defined as the time required for the intensity to be reduced to half its original value.

In summary, the size dependences of the PL and CL properties of $Y_2O_3S:Eu$ phosphors were examined. $Y_2O_3S:Eu$ phosphors of various particle sizes were synthesized by varying both the firing temperature and the firing time. The sizes of the $Y_2O_3S:Eu$ particles increase with increases in firing temperature and firing time. The larger $Y_2O_3S:Eu$ particles exhibit better PL properties. The PLE spectra consist of extremely broad bands that extend well into the near-UV region. Therefore, $Y_2O_3S:Eu$ can be used as a red-emitting phosphor in three-band white LEDs excited by near-UV LEDs. CL measurements of the $Y_2O_3S:Eu$ phosphor at middle voltages (3-8 kV) were performed to test its usefulness in CNT-FEDs. The CL brightness of the $Y_2O_3S:Eu$ phosphors was found to be independent of their particle size. The CL of $Y_2O_3S:Eu$ obtained at 1250 °C for 4 h is 534.5 cd/m^2 , for an applied voltage of 5 kV and a current density of 3 $\mu\text{A}/\text{cm}^2$. This is above the value of 460 cd/m^2 that is the requirement for CNT-FEDs. Therefore, $Y_2O_3S:Eu$ is an excellent red-emitting phosphor for middle voltage CNT-FEDs.

Conclusion

The dependence of the PL and CL properties of $Y_2O_3S:Eu$ phosphors on particle size were investigated. The sizes of the $Y_2O_3S:Eu$ particles increase with increases in firing temperature and firing time. The ratio of surface area to phosphor volume decreases with the increase in phosphor size. Surface defects produce nonradiative recombination processes of electrons and holes. Therefore, the PL efficiency is expected to increase as the particle size increases. However, the dependence of the particle size on CL brightness is

different from that on PL efficiency. The calculated penetration depths for the Y_2O_3S crystal at 5 keV is only 147 nm. The particle size produced at 1250 °C for 4 h is 5 μm . Since the penetration depth is much less than the particle size, most of the volume in the phosphor is not excited by electrons. Since small particles can be packed more densely than large particles, small particles have more volume excited by electrons and produce brighter intensity than those of large particles. This compensates for negative surface defect effect of small particles. Therefore, the CL brightness of a $Y_2O_3S:Eu$ phosphors at middle voltages (3-8 kV) is independent of particle size. $Y_2O_3S:Eu$ has excellent PL and CL properties that make it useful as a red-emitting phosphor in three-band white LEDs and CNT-FEDs.

Acknowledgment. This work was supported by the Ministry of Commerce, Industry and Energy of Korea through a Components and Materials Technology Development project (No. 0401-DD2-0162). This work was also supported by a grant number 2005-02522 (M10503000255-05M0300-25510) from the Nano R&D Program of the Ministry of Science and Technology. We also thank to the Brain Korea 21 project.

References

1. Kottaisamy, M.; Horikawa, H.; Kominami, H.; Aoki, T.; Azuma, N.; Nakamura, T.; Nakanishi, Y.; Hatanaka, Y. *J. Electrochem. Soc.* **2000**, *147*, 1612.
2. Lo, C. L.; Duh, J. G.; Chiou, B. S. *J. Electrochem. Soc.* **2002**, *149*, H129.
3. Mho, S. I.; Chang, S. Y.; Jeon, C. I.; Pyun, C. H.; Choi, Q. W.; Kim, C. H. *Bull. Kor. Chem. Soc.* **1990**, *11*, 386.
4. Park, S. H.; Mho, S. I.; Lee, K. W. *Bull. Kor. Chem. Soc.* **1996**, *17*, 487.
5. Hoffmann, U.; Weber, A.; Klages, C. P.; Mathee, T. *Carbon* **1999**, *37*, 753.
6. Shi, Y. S.; Zhu, C. C.; Qikun, W.; Xin, L. *Diam. Rel. Mater.* **2003**, *12*, 1449.
7. Kim, J. M.; Choi, W. B.; Lee, N. S.; Jung, J. E. *Diam. Rel. Mater.* **2000**, *9*, 1184.
8. Nakamura, S. *Solid State Commun.* **1997**, *102*, 237.
9. Yum, J. H.; Seo, S. Y.; Lee, S.; Sung, Y. E. *J. Electrochem. Soc.* **2003**, *150*, H47.
10. Schlotter, P.; Schmidt, R.; Schneider, J. *Appl. Phys. A* **1997**, *64*, 417.
11. Huh, Y. D.; Cho, Y. S.; Do, Y. R. *Bull. Kor. Chem. Soc.* **2002**, *23*, 1435.
12. Sato, Y.; Takahashi, N.; Sato, S. *Jpn. J. Appl. Phys. Part 2* **1996**, *35*, L838.
13. Chou, T. W.; Mylswamy, S.; Liu, R. S.; Chuang, S. Z. *Solid State Commun.* **2005**, *136*, 205.
14. Weast, R. C. *Handbook of Chemistry and Physics*, 70th ed.; 1989; F-187.
15. Lo, C. L.; Duh, J. G.; Chiou, B. S.; Peng, C. C.; Ozawa, L. *Mater. Chem. Phys.* **2001**, *71*, 179.
16. Tseng, Y. H.; Chiou, B. S.; Peng, C. C.; Ozawa, L. *Thin Solids Films* **1998**, *330*, 173.
17. Robert, A. R.; Fisher, J. F. *Television Engineering Handbook*; McGraw-Hill, New York, 1986.
18. Ozawa, L. *Cathodoluminescence Theory and Application*; VCH: New York, 1990; p 35.
19. Feldman, C. *Phys. Rev.* **1960**, *117*, 455.